Journal of Hazardous Materials 178 (2010) 693–698

Contents lists available at ScienceDirect

Journal of Hazardous Materials

journal homepage: www.elsevier.com/locate/jhazmat

Variable products in dielectric-barrier discharge assisted benzene oxidation

G.R. Dey, Asmita Sharma, K.K. Pushpa, Tomi Nath Das*

Radiation & Photochemistry Division, Bhabha Atomic Research Centre, Trombay, Mumbai 400085, India

ARTICLE INFO

Article history:
Received 19 October 2009
Received in revised form 29 January 2010
Accepted 29 January 2010
Available online 4 February 2010

Keywords:
Product control
Benzene oxidation
Phenyl radical
Dielectric-barrier discharge
Molecular sieve 10X
Phenol and substituted phenols

ABSTRACT

Atmospheric-pressure dielectric-barrier discharge (DBD) assisted control of benzene$_{(g)}$ oxidation into different classes of products is presented in this study. The gas-phase products were directly analyzed online by GC–FID and GC–MS. In addition, a solid yellowish surface deposit also formed, which was dissolved in 10 mL ethanol after each 10 min DBD cycle for GC analyses. One of the gas-phase products, phenol was also separately collected and estimated by *Folin–Ciocalteu's* wet-colorimetric method. In the gas phase only phenol and biphenyl were detected at maximum total conversion of ~3%, while in the ethanolic solution furthermore 1,2- and 1,4-dihydroxybenzene, 2,2′-biphenol, 2- and 4-phenylphenol and 4-phenoxyphenol were estimated at μM to mM level, and reveal ~30% total conversion. Products' types hint at the phenyl radical as the primary precursor. However, with the use of mesoporous molecular sieve 10X packing in unison with DBD, while the concentrations of such phenolic products decreased drastically, a number of open chain and non-aromatic ethers, aldehydes and esters, and also naphthalene and biphenylene were formed. In addition to high DBD process efficiency, the latter results suggest modification of discharge characteristics, and also strong physicochemical effects of cavity size and surface property on the intermediate reactions therein. Thus, use of such packing highlights a novel and practical methodology for control of chemical reactions towards useful product types, vis-à-vis pollutant mitigation.

1. Introduction

Efficient and diverse product generation in gas-phase benzene oxidation with dielectric-barrier discharge (DBD, *i.e.* cold plasma), in the absence and presence of mesoporous molecular sieve 10X (MS10X) packing is presented in this study. In the past, a variety of energy sources, *e.g.* thermal, UV light, ionizing radiation, ultrasonolysis, cold plasma without or with catalysts have been used to oxidize various aromatics including benzene [1–10]. But these studies in condensed matrices still lack details of the gas-phase or near-surface free radical reactions, as encountered in pollution. Conversely, the simple but versatile DBD technology has grown steadily to contribute in free radical mediated gas-phase chemical conversions [11–20]. However, with respect to pollution, these have mainly focused on complete oxidation of organics into CO_2 and H_2O, which may not only aggravate the non-desirable environmental effects, but also serve little as utility. Therefore, to evaluate the appropriate tunability and usage of the DBD process, oxidation of 500–10,000 ppm (1%) benzene (a typical aromatic) in Ar carrier with 2–40% O_2 was studied. Effective ~30% conversion of benzene into a variety of products was confirmed with gas chromatographic (GC) analysis, and plausible reaction mechanisms are presented. More significantly, while phenol and biphenyl were always produced, their further conversion to a mixture of substituted phenols in the absence of MS10X changed to a mixture of open chain and non-aromatic ethers, aldehydes and esters, etc. in its presence. Results suggest DBD with such packing may open up new avenues to contribute in the current efforts of tuning of a pollutant's alteration towards usable products vis-à-vis its mitigation.

2. Experimental

A 50 Hz DBD setup is shown in Fig. 1, and described before was employed for these measurements [21]. The annular discharge zone (gap 3.2 mm, volume 22 mL) is enclosed within electrically charged concentric *pyrex* surfaces. The applied voltage was varied from 2 to 10 kV. Carrier Ar:O_2 flow ratio was changed, with total flow rate maintained at 275 ± 45 mL min^{-1}. When needed, the annular gap was packed with activated MS10X globules (diameter 2–3 mm, obtained from M/s Union Carbide). Benzene (≥99% purity, from Spectrochem, India) concentration was altered by diverting a fraction of Ar (or O_2) flow through liquid C_6H_6 at constant temperature, and subsequently mixing it with the remaining gas flow prior to DBD. Gas-phase benzene concentration was measured at 254.6 nm ($\varepsilon = 210\ M^{-1}\ cm^{-1}$) in a 10 cm path cell [22]. The DBD outlet gas was sampled and analyzed by GC–FID (gas chromatograph–flame

* Corresponding author. Tel.: +91 22 25595097; fax: +91 22 25505151.
E-mail address: tndas@barc.gov.in (T.N. Das).

0304-3894/$ – see front matter © 2010 Elsevier B.V. All rights reserved.
doi:10.1016/j.jhazmat.2010.01.143

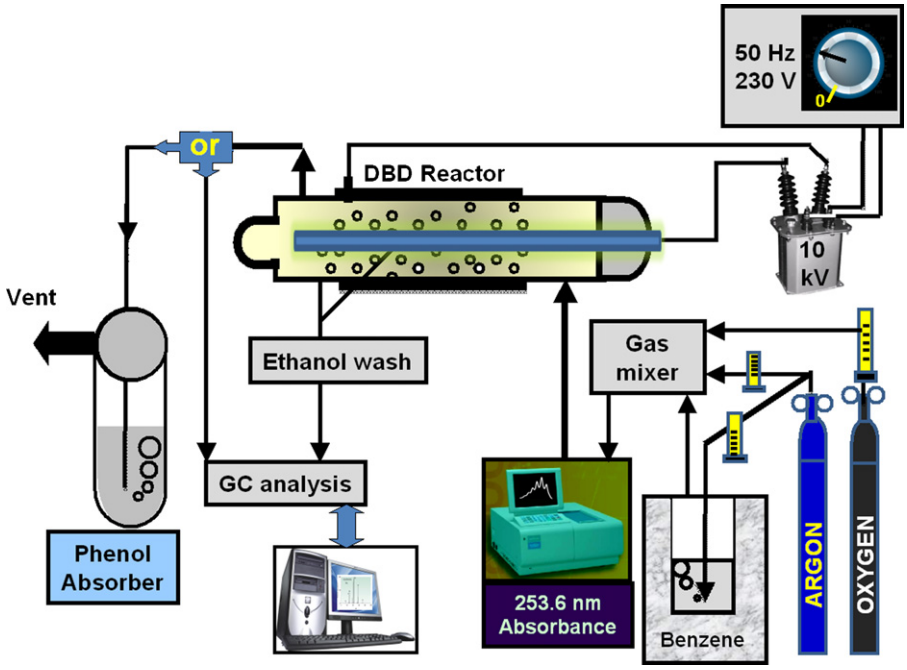

Fig. 1. DBD experimental set up with product analysis protocols.

ionization detector) and GC–MS (gas chromatograph–mass spectrometer) with BPX50 30 m × 0.25 mm ID capillary column, flow at 1.5 mL min^{-1}, temperature programming: 60 °C-r(10)-180, and in some cases by *Folin–Ciocalteu's* (FC) colorimetric analysis [23,24]. In addition, after each DBD cycle, a straw yellow colored deposited on each electrode surface were washed with 10 mL ethanol, and separately subjected to GC and GC–MS analyses. These analyses were made on Shimadzu 2010 series instrument. In quantitative GC–FID analysis, individual calibration plots were first obtained using pure standard samples. Subsequently, a comparison of the concerned experimental product's peak area with its standard's plot at the respective retention time revealed its prevailing concentration. The mass spectrometric (MS) fragmentation patterns at matching peak retention times were also checked and compared with the standard listings of NIST and Wiley Mass Libraries. The error in colorimetric and GC analyses remained within ±5%.

3. Results and discussion

3.1. Gas-phase studies

Keeping into perspective the report of phenol production in some previous condensed phase studies [5,25–32] the same was verified first. In Fig. 2a typical GC result shows gas-phase products collected for 10 min, by cooling in a liquid N_2-ethanol slurry bath at −116 °C [33]. In Fig. 2 inset results from FC measurements are shown, wherein $[phenol]_{aq}$ is presented in ppm taking into account the prevailing experimental parameters wherein the typical gas sampling rate was 240 mL min^{-1} for 10 min through 10 mL FC solution at 25 °C. Measurements under 6 kV applied voltage and flow rate at 240 mL min^{-1} revealed an averaged slope ≈2.4×10^{-3} for $[C_6H_5OH]_g$:$[C_6H_6]_g$. Under wide-ranging experimental conditions, [phenol] varied from 0.2 to 40 ppm, correlating to the conversion of 0.1–3% (maximum).

As listed in Table 1 (and compared in Fig. 2), with increasing $[O_2]$ up to ≤10%, phenol production increased continuously but decreased at higher $[O_2]$, possibly due to further oxidation of a fraction of phenol generated within the reaction zone. Herein GC analysis also revealed that [biphenyl] at low (2%) $[O_2]$ rapidly

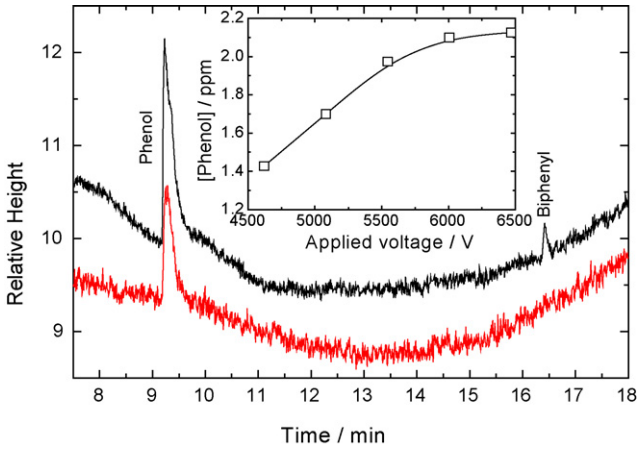

Fig. 2. Gas chromatogram of products collected for 25 min DBD at 7.7 kV applied voltage. Ar flow rate 260 mL min^{-1}, O_2 flow rate through C_6H_6 at 0° C: (a) 28 mL min^{-1} (*black curve*) and (b) 65 mL min^{-1} (*red curve*). *Inset*: Gas-phase phenol concentration estimated using the wet-chemical method *vs.* applied voltage. Total gas flow rate: 265 mL min^{-1}, O_2 flow rate 7.5%, Ar flow rate through C_6H_6 at 0 °C: 24 mL min^{-1}.

decreased with increasing $[O_2]$, and its inverse relation to [phenol] as shown in Table 1. To rationalize the chemistry, a set of plausible sequential reaction mechanism (1)–(19) is postulated to occur. (In these studies Ar and O_2 were used as the carrier and oxidizer

Table 1
Dependency of phenol and biphenyl generation on oxygen concentration for total gas flow rate: 240 mL min^{-1}, DBD at 7.4 kV applied voltage, $[C_6H_6]$ = 1500 ppm.

O_2 (%)	Phenol generated (ppm)	Biphenyl generated (ppb)
2–3	19	–
6.2	22	13
8.6	24	0.7
10	25.5	0.3
11.5	25	BDL
24	12	BDL
40	7	BDL

BDL = below detection limit

respectively to avoid any complication arising out of N-atom and various N_xO_y radicals and subsequent products reported in 78-21 mixture of $N_2 + O_2$ (mimicking air) under DBD.)

Energy absorption:

$$Ar \xrightarrow{DBD} Ar^* + Ar_n^{\bullet+} \ (n = 1 \text{ and } 2) + e^- \quad (1)$$

$$O_2 \xrightarrow{DBD} O_2^* \quad (2)$$

Primary reactions:

$$Ar* + O_2 \rightarrow O_2* + Ar \quad (3)$$

$$O_2* \rightarrow 2O \quad (4)$$

$$Ar* + C_6H_6 \rightarrow C_6H_6* + Ar \quad (5)$$

$$Ar_n^{\bullet+} + C_6H_6 \rightarrow C_6H_6^{\bullet+} + nAr \quad (6)$$

Secondary reactions:

$$C_6H_6* \rightarrow C_6H_5^{\bullet} + H^{\bullet} \quad (7)$$

$$O_2 + O(+Ar) \rightarrow O_3(+Ar) \quad (8)$$

$$O + C_6H_6 \rightarrow C_6H_5^{\bullet} + {}^{\bullet}OH \quad (9)$$

Further reactions:

$$C_6H_5^{\bullet} + C_6H_5^{\bullet} \rightarrow \mathbf{C_6H_5{-}H_5C_6}(\text{biphenyl}) \quad (10)$$

$$C_6H_5^{\bullet} + O_2 \rightarrow C_6H_5O_2^{\bullet}(\text{phenylperoxylradical}) \rightarrow \mathbf{C_6H_5OH}(\text{phenol}) \quad (11)$$

$$C_6H_6 + {}^{\bullet}OH \longrightarrow C_6H_6{}^{\bullet}OH \xrightarrow{(O_2)} \mathbf{C_6H_5OH} \ (+ HO_2^{\bullet}) \quad (12)$$

$$H^{\bullet} + O_2 \rightarrow HO_2^{\bullet} \quad (13)$$

$$C_6H_6^{\bullet+} + mC_6H_6 \rightarrow (C_6H_6)_{m+1}^{\bullet+} \rightarrow \mathbf{polymeric products} \quad (14)$$

$$C_6H_5^{\bullet} + mC_6H_6 \rightarrow \mathbf{(C_6H_6)_mH_5C_6^{\bullet}} \rightarrow \mathbf{polymeric products} \quad (15)$$

Minor reactions:

$$C_6H_5^{\bullet} + {}^{\bullet}OH \rightarrow \mathbf{C_6H_5OH} \quad (16)$$

$${}^{\bullet}OH + {}^{\bullet}OH \rightarrow \mathbf{H_2O_2} \quad (17)$$

$$HO_2^{\bullet} + HO_2^{\bullet} \rightarrow \mathbf{H_2O_2 + O_2} \quad (18)$$

Additional reaction in the presence of excess oxygen:

$$O_2* + C_6H_6 \rightarrow C_6H_6* + \mathbf{O_2} \quad (19)$$

Composition of the flowing reaction mixtures would allow initial DBD energy partition mainly between Ar and O_2 as in reactions (1) and (2) (a negligible fraction may be absorbed by the C_6H_6 present). As a result, in addition to $Ar^* + Ar_n^{\bullet+}$, other chemically reactive species formed include the O-atom, and subsequently O_3, $C_6H_5^{\bullet}$ and $C_6H_6^{\bullet+}$ radicals, each following its separate chemistry.

The O-atom reactions fall in three categories, reaction (8) to generate ozone, reaction (9) to generate the $C_6H_5^{\bullet}$ and ${}^{\bullet}OH$ radicals, and its radical recombination (not shown) to regenerate O_2. Gas-phase reactions of O_3 and C_6H_6 are discussed elsewhere in the literature [34,35]. The $C_6H_5^{\bullet}$ radical reaction propensities would have minor, intermediate, and major contributions in the above scheme. In the minor category, the reaction (not shown above) deals with its internal rearrangement, leading to open-chain products, which may however gain importance under restricted reaction environment, discussed later. Following the major channels, the reactions are initiated as shown above in (10), (11) and (15). The bimolecular rate constant of radical dimerization reaction (10) in the gas phase is reported to be 1.15×10^{13} mL^3 mol^{-1} s^{-1} [36]. Therefore, its overall contribution in defining the various product ratios depends on the absence of other majority reactants that also scavenge the $C_6H_5^{\bullet}$ radical. Herein such scavengers are O_2 and the parent C_6H_6. The propensity of the scavenging reactions (11) and (15) remain high due to prevailing extremely high ratios of the $[O_2]$:$[C_6H_5^{\bullet}]$ and $[C_6H_6]$:$[C_6H_5^{\bullet}]$. The bimolecular rate constant of initiation of reaction (15) at 298 K is reported to be high, $k = 1.81 \times 10^9$ mL^3 mol^{-1} s^{-1} [37]. Although a similar initiation by $C_6H_6^{\bullet+}$ in reaction (14) has not yet been quantified, its consequences under DBD may be of similar magnitude due to high $[C_6H_6]$:$[C_6H_6^{\bullet+}]$ ratio arising out of reactions (1) and (6). Thus, in the presence of ppm level C_6H_6 in the gas stream, the combined contribution of reactions (14) and (15) would remain significant, as observed in this study. It may be noted that at 298 K the reaction rate constant value of $C_6H_5^{\bullet} + C_6H_6 \rightarrow H^{\bullet} + C_6H_5{-}H_5C_6$ is reported to be 4.65×10^8 mL^3 mol^{-1} s^{-1} [38]. Thus yield of biphenyl reactions (13) and (18) propensities would increase following it.

In the condensed phase some substituted phenylperoxyl radicals (*sub*-$C_6H_4O_2^{\bullet}$) are reported to generate the corresponding phenoxyl radical (*sub*-$C_6H_4O^{\bullet}$) via the diphenyltetroxide (*sub*-$C_6H_4OOOOH_4$(*sub*-)C_6) intermediate in respective dimerization reactions [39]. Even in the gas-phase reactions near room temperature a similar reaction is reported to occur [40]. On the other hand, at higher temperatures, a similar direct reaction, $C_6H_5^{\bullet} + O_2 \xrightarrow{-(Ar)} C_6H_5O^{\bullet} + O$ has been reported, without the intermediacy of its tetroxide ($C_6H_5OOOOH_5C_6$) [41]. Thus, under DBD conditions, in reaction (11) the phenylperoxyl radical, $C_6H_5O_2^{\bullet}$ may generate the $C_6H_5O^{\bullet}$ radical via the tetroxide, *i.e.* $2C_6H_5{-}O_2^{\bullet} \rightarrow [C_6H_5O_2{-}O_2H_5C_6] \rightarrow 2C_6H_5O^{\bullet} + O_2$. A similar reaction scheme has been proposed recently [8]. The latter is expected to get reduced to phenol by abstracting an H-atom from a suitably abundant source like C_6H_6 in the present case [42], $C_6H_5O^{\bullet} + C_6H_6 \rightarrow C_6H_5OH + C_6H_5^{\bullet}$, and starting the reaction cycle all over again. Formation of a stronger O–H bond in lieu of a weaker C–H bond would favor such an H-atom abstraction reaction in this case.

While the radical–radical addition reaction (16) possibly falls in the minor category (due to prevailing low concentration of the either species, thus may arise only from a geminate recombination of reaction (9) products), oxygenation of the ${}^{\bullet}OH$ adduct in reaction (12) would be an important channel for phenol generation. Similar reaction mechanism in condensed phase is reported in the literature [43]. The sequential steps in it are (a) formation of the 5-hydroxy-(1,3)-cyclohexadienyl radical, $C_6H_6{}^{\bullet}OH$; (b) addition of O_2 at C_6 generating the corresponding peroxyl radical, $HOC_6H_6O_2^{\bullet}$; and (c) elimination of the hydroperoxy radical, $HO_2^{\bullet}$ (O_2 from C_6 with H from C_5) generating phenol, C_6H_5OH.

Some additional reactions, *e.g.* of $H^{\bullet}$ from reaction (7) with O_2 and C_6H_6 may also produce the $HO_2^{\bullet}$ (reaction (13)) and $C_6H_7^{\bullet}$ (not shown) radicals respectively, and further chemistry may occur. As discussed later, within restricted environments (and if $H^{\bullet}$ is not allowed to be scavenged by O_2) the latter reaction may gain significance and thereby lead to ring opening and further addition of oxygen to produce open-chain products. Additionally, within the discharge zone, reaction (17) may become reversible, at least partially to maintain a steady concentration of the ${}^{\bullet}OH$ radical. Thus, along with the presence of some minor reactions, generation of majority phenol and biphenyl in the gas stream is rationalized, including their inverse relation vis-à-vis presence of O_2. For an experimental residence time of ~5 s in the reaction zone, comparable lower concentration levels of either product would also ensure their minimal degradation under DBD. Thus, the measured gas-phase concentrations of these species are assumed to remain unaffected.

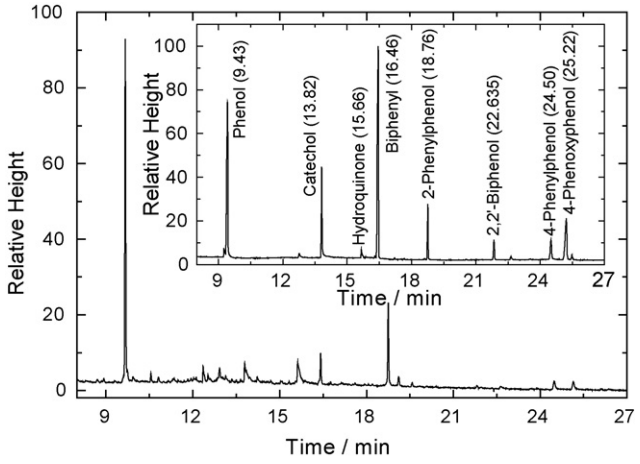

Fig. 3. Gas chromatogram of surface washed ethanolic solution from 10 min DBD at 7.7 kV applied voltage, Ar flow rate: 217 mL min^{-1}, Ar flow rate through C_6H_6 at 0 °C: 40 mL min^{-1}, with 8% O_2. *Inset*: Gas chromatogram of ethanolic solution of μM to mM of various standards employed.

Table 2
Typical products estimated (in μmol) in 10 mL of ethanolic solutions under 10 min DBD at 8.4 kV applied voltage. Ar flow rate: 240 mL min^{-1}; [C_6H_6] = 1150 ppm and [O_2] = 20%.

Product	Without MS10X	With MS10X
Phenol	1.65	0.48
Biphenyl	0.047	0.12
2- and 4-phenylphenols	0.18	0.024
Catechol	0.22	Nil
2,2′-Biphenol	0.026	Nil
4-Phenoxyphenol	0.045	Nil
Hydroquinone	1.5	Nil

GC analysis of an ethanolic wash in Fig. 3 reveals major phenol and biphenyl (with significantly higher yields as compared to gas phase) peaks, and also hydroquinone, catechol, 2,2′-biphenol, 4-phenoxyphenol, 2- and 4-phenylphenols, etc. and a few minor unidentified species. Detailed analyses also revealed that herein too [biphenyl] were inversely related to [O_2] (0.048 μM to nil for 4% to 10% O_2 respectively), and [phenol] as found earlier. A typical estimate of the product yields is listed in Table 2 (under without MS10X). FC measurements additionally revealed that deposited $[\text{phenolic}]_{total}$ was $\geq 10 \times [\text{phenol}]_{gas}$. The deposited products suggest the following: (a) significant (near-electrode) surface chemistry during DBD, wherein not only the reactions (1)–(18) but additional chemistry as discussed in Scheme 1 and beyond (such as the mechanism discussed by Gai [44]) may take place continuously; (b) polymeric products from reactions (14) and (15) may continue to get deposited on the dielectric surfaces due to low vapor pressure. Various chemicals and the discharge close to the surface further modify such deposits. Thus, some of the phenolic compounds may be formed as later reaction products, from the polymer breakdown, followed by oxygenation of its daughter fragments. Such reaction mechanisms are discussed below.

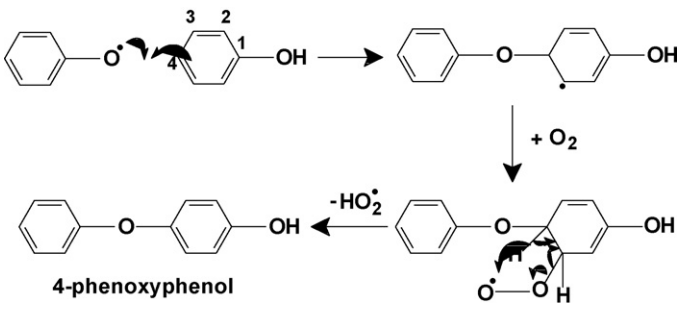

Scheme 1.

Table 3
Comparison of various products (with retention time) identified in the ethanol washed solutions of MS10X globules during DBD modification of C_6H_6 in the presence of low and high concentrations of O_2 (common products are shown in bold).

2% O_2	14% O_2
(1-Methylethenyl)benzene (8.87)	5-Hydroxymethyl-2-furanone (6.22)
(Methylphenylacetyl)-benzene (10.55)	2-Cyclohexene-1-ol (7.72)
3-Phenyl-2-propanal (11.27)	**(1-Methylethenyl)benzene (8.90)**
Aceticacid phenyl ester (11.73)	2-Cyclopentene-1,4-dione (9.28)
3-Phenyl-2-propenal (12.29)	Diethyl ethanedionic acid (10.04)
Naphthalene (13.50)	3,4-Dihydropyran (10.40)
(2,5-Cyclohexadienyl)benzene (14.91)	**(Methylphenylacetyl)-benene (10.55)**
(1,4-Cyclohexadienyl)benzene (15.33)	Phenylpentanoic acid (11.28)
Diphenylether (16.76)	Ethyl-trans-2-pentenoate (11.76)
Biphenylene (17.60)	2-Methylene-1-propionyl cyclopropane (12.51)
2-Phenoxyphenol	3,4-Dimethyl-2-cyclohexene-1-one (14.23)

Presence of various 2- and 4-substituted phenolic products may be rationalized by assuming their formation to occur from phenol that is first generated on or near the surfaces, and subsequently gets deposited. Taking the example of 4-phenoxyphenol generation, the plausible sequential reactions are shown in Scheme 1. (It may be noted that a similar $C_6H_5O^\bullet$ attack occurring at C_2 would generate 2-phenoxyphenol, especially under a restrictive environment as discussed later and shown in Table 3, while replacing the $C_6H_5O^\bullet$ with $C_6H_5^\bullet$ would produce the respective phenylphenol in either case.) Preferential 2- and 4-(electrophilic) substitutions of either $C_6H_5O^\bullet$ or $C_6H_5^\bullet$ radicals occur at the centers of highest electron density, *i.e.* C_2 and C_4 in phenol. The reaction mechanism in Scheme 1 is similar to the oxidation of aqueous solution of C_6H_6 in the presence of $^\bullet$OH radical and dissolved O_2 [4].

On the other hand, 2,2′-biphenol could be generated from (a) surface deposited biphenyl by sequential $^\bullet$OH radical addition, followed by O_2 addition, and $HO_2^\bullet$ radical elimination twice over on either ring; or (b) from phenylphenols by appropriate sequential $^\bullet$OH radical addition, O_2 addition, $HO_2^\bullet$ radical elimination. In either case electron density distribution in the intermediate species would determine the course of such reactions, thus preventing formation of other isomers. Even generation of catechol and hydroquinone from phenol would follow similar chemistry or mechanism starting with phenol and/or C_6H_6. Thus, although the presence of O_2 is crucial for C_6H_6 oxidation, under DBD, its prevailing high concentration plausibly allows continuous generation of the $^\bullet$OH radical via the reactions (3), (4) and (9), leading to production of above secondary and tertiary reaction products. Additionally, O_3 present may also play a crucial role in such chemistry. To verify this hypothesis the experimental design was modified to allow (a) production of only O_3 under DBD (employing O_2 in carrier argon), and later mixing it with C_6H_6 in Ar; and (b) by treating the polymeric deposit formed first (employing benzene in carrier argon in the absence of O_2) with O_3 generated separately. However, under these conditions formation of such coating in the first case, and formation of any substituted phenol in the second case was found to be negligible. Thus, in our studies role of O_3 in this direction possibly remained low, supporting the above reaction sequence.

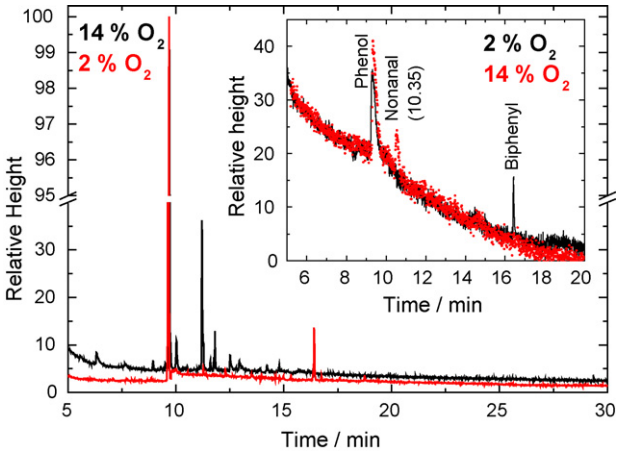

Fig. 4. Gas chromatogram of products ethanol washed from MS10X for 20 min DBD at 9 kV applied voltage. For 2% O_2: total gas flow rate 300 mL min^{-1} and Ar flow rate through C_6H_6 in ice-water bath: 50 mL min^{-1}. For 14% O_2: total gas flow rate: 265 mL min^{-1}; Ar flow rate through C_6H_6 in ice-water bath: 43 mL min^{-1}. *Inset*: Gas chromatogram of gas-phase products obtained from 10 min DBD under 9 kV applied voltage, with MS10X packing at different O_2 concentrations. In either case total gas flow rate: 300 mL min^{-1}; Ar flow rate through C_6H_6 at 0 °C: 50 mL min^{-1}.

3.2. Reactions in the presence of MS10X packing

The GC–MS analysis of gas-phase products in Fig. 4 inset again confirmed that phenol and biphenyl were produced in the presence of low [O_2], but production of nonanal $C_8H_{17}CHO$ (and absence of biphenyl) at high [O_2] clearly showed a significant deviation from the previous oxidation route (with ring opening, addition of a C_3 moiety, partial hydrogenation, and an oxygenation step).

In GC analyses of the ethanolic wash of MS10X globules, various hydrocarbons and oxygenated species were identified as products. In Table 3 a partial list products formed in the presence of 2% and 14% [O_2] is presented. (A complete list of products appears in the Supporting information Table S1.) The chromatogram in Fig. 4 for 2% [O_2] show products biphenyl, naphthalene, cyclohexadienyl and other substituted benzenes, biphenylene, and some oxygenated species like phenol, diphenyl ether, and a number of single ring or open-chain species. At higher [O_2] most of the hydrocarbon products (and the various phenolic species found without MS10X) were absent. Instead various new non-aromatic species with higher oxygen content were formed. Diverse nature of such products resulted from the combination of DBD and MS10X packing, which significantly modified the oxidative process as a result of changes in the micro-discharge properties. Instead of a volume discharge (absence of MS10X), a multitude of surface discharges occurred on/near the pellets, with micro-plasmas in the interstices between pellets, which strongly influenced the discharge physics and the chemical reactions within the discharge gap.

The mesoporous calcium aluminosilicate network in MS10X has ~7.8 Å apertures and ~13 Å cavity diameters, and thus would allow entry and retention of appropriate size molecules within it for different lengths of times. These categories of materials are well recognized for catalytic and adsorption properties [45]. The large area of granular surface would help some skimming molecules to enter into the crevices within, remain entrapped and get chemically affected disparately. Depending on their size and shape, the absorbed/adsorbed molecules, or even some reaction products may also traverse dissimilar paths, get segregated, and remain entrapped for different lengths of time, and get repeatedly affected by DBD energy. Thus, continuous but dissimilar transformations ensue; opposite of the case when the packing is absent, and residence time too short for such secondary effects, suggesting an overall complex chemical process in the presence of MS10X.

The molecular size of C_6H_6 (~5 Å *para* H-atoms' distance) would allow its facile entry into the MS10X channels and cavities. The cavity size would even permit simultaneous entry and residence of (maximum) two C_6H_6 molecules within it. Therefore under DBD, various reactions would ensue. For example, when two C_6H_6 molecules get entrapped together in the same cavity, these may loose one or even more H-atoms in reactions similar to 7. Radical centers resulting from these initial H-atom losses would be the subsequent sites for ring-attachments or other bonding(s) via radical-radical and/or radical–non-radical chemistry. As a result, products like biphenyl (either C_6H_6 molecule looses one H-atom followed by radical dimerization), diphenyl ether (with an intervening O-atom generated following reaction (4) generated elsewhere or within the same cavity), or even biphenylene (when either C_6H_6 molecule looses two H-atoms, especially in the absence of O_2) would form. If one C_6H_6 molecule gets fragmented (cleavage of C=C bond when excess energy is absorbed), naphthalene would be generated after appropriate attachments (one C_6H_6 molecule looses two H-atoms, the other is fragmented into a C_4 moiety). The H-atoms generated therein [42] are either expected to desorb as H_2 or relocate or participate in hydrogenation reactions, thereby partially saturating a few C=H bonds in subsequent products formed. Variety of oxygenation reactions are also expected to gain importance in the presence of increasing amounts of O_2, in addition to partial removal of some H-atom fragments generated. Some of the reaction products forming in the presence of low [O_2] would therefore get masked. Additionally, a variety of cleaved moieties with one to six C-atoms are also expected to react with O_2 to form open-chain, aliphatic oxidized products like alcohols, acids, esters, or even closed ring ethers. Interestingly, during long-time DBD (1 h or more) in the absence of MS10X, naphthalene, biphenylene, diphenyl ether, etc. were also observed, suggesting their formation in later reactions within/on the organic deposits.

To further narrow down the product range to any specific type vis-à-vis the wide range of primary reactions species observed above, detailed and systematic studies on different aspects of the physicochemical effects (*i.e.* change in physical parameters like cell geometry, cell length, packing cavity size, discharge characteristics including its frequency, and duration, etc.) are mandatory, and are underway. However, the relevance and utility of MS10X packing in unison with DBD may be judged from the fact that phenolic compounds are known to be stronger health hazards as compared to some of the other open-chain products listed above. Interestingly, irrespective of the physical conditions employed, phenol was always identified as the major product (~70%) in C_6H_6 oxidation. Correlation with the input electrical energy parameters reveals that a maximum of ~30% oxidation/degradation of C_6H_6 was achievable in these measurements.

4. Conclusion

Gas-phase DBD assisted benzene$_{(g)}$ oxidation produces phenol and substituted phenols in addition to biphenyl, both in the gas phase and as surface deposited products, suggesting the intermediacy of the phenyl radical as the primary precursor. While a maximum gas-phase conversion of ~3% was achieved, ~30% total conversion was measured including the surface conversions. However, with MS10X packing within the reaction zone, various open-chain and multi-oxygenated compounds or polynuclear aromatics were formed in lieu of the above products. These measurements suggest possible user control and tuning of discharge characteristics and application of packing cavity size and surface property on the intermediate reactions therein, for potential management of products' type, vis-à-vis pollutant mitigation.

Acknowledgements

This research was carried out under the XIth Plan Sub-project 27_R&D_N_34.06. The authors thank DAE and BARC for the funding.

Appendix A. Supplementary data

Supplementary data associated with this article can be found, in the online version, at doi:10.1016/j.jhazmat.2010.01.143.

References

[1] C. Walling, R.A. Johnson, Fenton's reagent. V. Hydroxylation and side-chain cleavage of aromatics, J. Am. Chem. Soc. 97 (1975) 363–367.
[2] J. Zhong, J. Wang, L. Tao, M. Gong, L. Zhimin, Y. Chen, Photocatalytic degradation of gaseous benzene over TiO_2/Sr_2CeO_4: kinetic model and degradation mechanisms, J. Hazard. Mater. 139 (2007) 323–331.
[3] J.D. Coates, R. Chakraborty, J.G. Lack, S. O'Connor, K.A. Cole, K.S. Bender, L.A. Achenbach, Anaerobic benzene oxidation coupled to nitrate reduction in pure culture by two strains of *Dechloromonas*, Nature 411 (2001) 1039–1043.
[4] H. Park, W. Choi, Photocatalytic conversion of benzene to phenol using modified TiO_2 and polyoxometalates, Catal. Today 101 (2005) 291–297.
[5] X.-M. Pan, M.N. Schuchmann, C. von Sonntag, Oxidation of benzene by the •OH radical. A product and pulse radiolysis study in oxygenated aqueous solution, J. Chem. Soc., Parkin Trans. 2 (1993) 289–297.
[6] O. Godoy-Cabrera, R. Lopez-Callejas, J.S. Benitez-Read, J.O. Pacheco-Sotelo, A. de la Piedad-Beneitez, Short-time sonolysis of chlorobenzene in the presence of Pd(II) salts and Pd(0), Int. J. Electron. 92 (2005) 327–340.
[7] C. Stavarache, M. Vinatoru, R. Nishimura, Y. Maeda, High-voltage and high-frequency inverter controlled by DPLL for cold plasma applications, Ultrason. Sonochem. 11 (2004) 429–434.
[8] D. Ascenzi, P. Franceschi, G. Guella, P. Tosi, Phenol production in benzene/air plasmas at atmospheric pressure. Role of radical and ionic routes, J. Phys. Chem. A 110 (2006) 7841–7847.
[9] Z. Ye, Y. Zhang, P. Li, L. Yang, R. Zhang, H. Hou, Feasibility of destruction of gaseous benzene with dielectric barrier discharge, J. Hazard. Mater. 156 (2008) 356–364.
[10] E. Hisahiro, O. Atsushi, Benzene oxidation with ozone over supported manganese oxide catalysts: effect of catalyst support and reaction conditions, J. Hazard. Mater. 164 (2009) 1236–1241.
[11] U. Kogelschatz, Dielectric-barrier discharges: their history, discharge physics, and industrial applications, Plasma Chem. Plasma Process. 23 (2003) 1–46.
[12] U. Kogelschatz, Atmospheric-pressure plasma technology, Plasma Phys. Control. Fusion 46 (2004) B63–B75.
[13] U. Kogelschatz, Twenty years of Hakone Symposia; from basic plasma chemistry to billion dollar markets, Plasma Process. Polym. 4 (2007) 678–781.
[14] H.-H. Kim, Nonthermal plasma processing for air-pollution control: a historical review, current issues, and future prospects, Plasma Process. Polym. 1 (2004) 91–110.
[15] S. Muller, R.-J. Zahn, Air pollution control by non-thermal plasma, Contrib. Plasma Phys. 47 (2007) 520–529.
[16] A. Ogata, N. Shintani, K. Mizuno, S. Kushiyama, T. Yamamoto, Decomposition of benzene using nonthermal plasma reactor packed with ferroelectric pellets, IEEE Trans. Ind. Appl. 35 (1999) 753–759.
[17] D.W. Park, S.H. Yoon, G.J. Kim, H. Sekiguchi, The Effect of catalyst on the decomposition of dilute benzene using dielectric barrier discharge, J. Ind. Eng. Chem. 8 (2002) 393–398.
[18] B.-Y. Lee, S.-H. Park, S.-C. Lee, M. Kang, S.-J. Choung, Decomposition of benzene by using a discharge plasma–photocatalyst hybrid system, Catal. Today 93–95 (2004) 769–776.
[19] H.-H. Kim, H. Korbara, A. Ogata, S. Futamura, Comparative assessment of different nonthermal plasma reactors on energy efficiency and aerosol formation from the decomposition of gas-phase benzene, IEEE Trans. Ind. Appl. 41 (2005) 206–214.
[20] B. Lu, X. Zhang, X. Yu, T. Feng, S. Yao, Catalytic oxidation of benzene using DBD corona discharges, J. Hazard. Mater. 137 (2006) 633–637.
[21] G.R. Dey, T.N. Das, Selective gas-phase and on-surface chemical reduction of CO_2 to CO and HCHO under dielectric barrier discharge, Plasma Chem. Plasma Process. 26 (2006) 495–505.
[22] H.R. Du, A. Fuh, J. Li, A. Corkan, J.S. Lindsey, PhotochemCAD: a computer-aided design and research tool in photochemistry, Photochem. Photobiol. 68 (1998) 141–142.
[23] O. Folin, V. Ciocalteu, On tyrosine and tryptophane determinations in proteins, J. Biol. Chem. 73 (1927) 627–650.
Folin–Ciocalteu's Colorimetric Analysis. The FC reagent was obtained locally from E. Merck. Presently the analytical protocols were standardized with μM to mM aqueous phenol solutions. Following it, subsequent to the reagent's reaction with phenol, 7% Na2CO3 was used for neutralization, and a deep blue color developed with its molar absorptivity, $\varepsilon = 7500\ M^{-1}\ cm^{-1}$ measured at $\lambda_{max} = 750$ nm. Ref: V.L. Singleton, J.A. Rossi, Jr., Colorimetry of total phenolics with phosphomolibdic-phosphothungstic acid, Am. J. Enol. Viticul., 16 (1965) 1441–1458.
[24] G.R. Dey, Significant roles of oxygen and unbound •OH radical in phenol formation during photo-catalytic degradation of benzene on TiO_2 suspension in aqueous solution, Res. Chem. Intermed. 35 (2009) 573–587.
[25] S. Mahapatra, R. Vinu, T.N.G. Row, G. Madras, Kinetics of photoconversion of cyclohexane and benzene by $LnVO_4$ and $LnMo0.15V0.85O_4$ (Ln = Ce, Pr and Nd), Appl. Catal. A: Gen. 351 (2008) 45–53.
[26] H. Ge, Y. Leng, F. Zhang, C. Zhou, J. Wang, Direct hydroxylation of benzene to phenol with molecular oxygen over pyridine-modified vanadium-substituted heteropoly acids, Catal. Lett. 124 (2008) 250–255.
[27] M.H. Sayyar, R.J. Wakeman, Comparing two new routes for benzene hydroxylation, Chem. Eng. Res. Des. 86 (2008) 517–526.
[28] S. Kwon, M. Fan, A.T. Cooper, H. Yang, Photocatalytic applications of micro- and nano-TiO_2, Environ. Eng. Crit. Rev. Environ. Sci. Technol. 38 (2008) 197–226.
[29] Y. Ichihashi, T. Taniguchi, H. Amano, T. Atsumi, S. Nishiyama, S. Tsuruya, Liquid-Phase oxidation of benzene to phenol by molecular oxygen over La catalysts supported on HZSM-5, Top. Catal. 47 (2008) 98–100.
[30] Y. Shuangfeng, W. Shuisheng, D. Weili, L. Wensheng, H. Mengguang, Z. Xiaoping, Direct phenol synthesis by catalytic oxidation of benzene with molecular oxygen, Prog. Chem. 19 (2007) 735–744.
[31] M. Tani, T. Sakamoto, S. Mita, S. Sakaguchi, Y. Ishii, Hydroxylation of benzene to phenol under air and carbon monoxide catalyzed by molybdovanadophosphoric acid, Angew. Chem. Int. Ed. 44 (2005) 2586–2588.
[32] S.-T. Yamaguchi, S. Sumimoto, Y. Ichihashi, S. Nishiyama, S. Tsuruya, Liquid-phase oxidation of benzene to phenol over V-substituted heteropolyacid catalysts, Ind. Eng. Chem. Res. 44 (2005) 1–7.
[33] R.E. Rondeau, Slush baths, J. Chem. Eng. Data 11 (1966) 124.
[34] C.T. Pate, R. Atkin, J.N. Pitts Jr., The gas phase reaction of O_3 with a series of aromatic hydrocarbon, J. Environ. Sci. Health A 11 (1976) 1–8.
[35] S. Toby, L.J. Van de Burgt, F.S. Toby, Kinetics and chemiluminescence of ozone-aromatic reactions in the gas phase, J. Phys. Chem. 89 (1985) 1982–1986.
[36] J. Park, M.C. Lin, Kinetics for the recombination of phenyl radicals, J. Phys. Chem. A 101 (1997) 14–18.
[37] M. Preidel, R. Zellner, A cw laser absorption study of the reactions of phenyl radicals with NO, NO_2, O_2 and selected organics between 298–404 K, Ber. Bunseng. Phys. Chem. 93 (1989) 1417–1423.
[38] A. Fahr, S.E. Stein, Reactions of vinyl and phenyl radicals with ethyne, ethene and benzene, in: 22nd International Symposium on Combustion, vol. 22, The Combustion Institute, Pittsburgh, 1989, pp. 1023–1029.
[39] G.I. Khaikin, Z.B. Alfassi, P. Neta, Inter- and intra-molecular redox reactions of substituted phenylperoxyl radicals in aqueous solutions, J. Phys. Chem. 99 (1995) 16722–16726.
[40] T. Yu, M.C. Lin, Kinetics of the $C_6H_5 + O_2$ reaction at low temperatures, J. Am. Chem. Soc. 116 (1994) 9571–9576.
[41] P. Frank, J. Herzler, Th. Just, C. Wahl, High-temperature reactions of phenyl oxidation, in: 25th International Symposium on Combustion, vol. 25, The Combustion Institute, Pittsburgh, 1994, pp. 833–840.
[42] N. Na, Y. Xia, Z. Zhu, X. Zhang, R.G. Cooks, Birch reduction of benzene in a low-temperature plasma, Angew. Chem. Int. Ed. 48 (2009) 2017–2019.
[43] E. Mvula, M.N. Schuchmann, C. von Sonntag, Reactions of phenol-OH-adduct radicals. Phenoxyl radical formation by water elimination vs. oxidation by dioxygen, J. Chem. Soc., Perkin Trans. 2 (2001) 264–268.
[44] K. Gai, Aqueous diphenyl degradation induced by plasma with glow discharge electrolysis, J. Chem. Chem. Soc. 53 (2006) 627–632.
[45] S. Inagaki, S. Guan, Y. Fukushima, T. Ohsuna, O. Terasaki, Novel mesoporous materials with a uniform distribution of organic groups and inorganic oxide in their frameworks, J. Am. Chem. Soc. 121 (1999) 9611–9614, and references therein.